



Spatio-temporal mangrove canopy variation (2001–2016) assessed using the MODIS enhanced vegetation index (EVI)

Marta Rocío Nepita-Villanueva¹ · César Alejandro Berlanga-Robles² · Arturo Ruiz-Luna² · J. Héctor Morales Barcenás³

Received: 15 January 2018 / Revised: 28 March 2019 / Accepted: 1 April 2019 / Published online: 11 April 2019
© Springer Nature B.V. 2019

Abstract

Variation patterns in mangrove canopies were evaluated for the Marismas Nacionales coastal ecosystem (northwest Mexico), based on a monthly time series (2001 to 2016) of the MODIS enhanced vegetation index (EVI). By using a non-centralized normalized principal component analysis (PCA), the imagery series was decomposed to the S and T modes, allowing the identification of recurrent temporal patterns as well as spatial patterns over time. It was found that the maximum vegetation vigor in mangroves occurs in autumn, 4–5 months after the driest season, while approximately 15% of the mangrove canopy displayed decreasing trends because of disturbance events, including anomalies in temperature and precipitation. Most of the mangrove canopy was stable (78%), while the remaining 7% was found to be in a recovery phase. The most vulnerable mangrove canopies were detected in areas defined in previous studies as dominated by *Avicenia germinans*, while resistant and resilient forests were located in areas dominated by *Laguncularia racemosa*.

Keywords Mangroves · MODIS · Enhanced vegetation index (EVI) · Time series · Principal component analysis (PCA)

Introduction

Coastal wetlands conservation and management strategies require accurate and updated information on their distribution and trends of change, which can be produced with the use of remote sensing data and techniques (Giri et al. 2011; Kuenzer et al. 2011; Giri 2016). Regarding mangroves, one of the most studied coastal wetlands, research based on satellite data analyses mainly uses medium to very high resolution optical products (Landsat, SPOT, ASTER, Ikonos). Recently, applications

with radar and LiDAR data in contextual analyses (e.g., classification with neural networks) have increased the potential of remote sensing for inventorying and monitoring mangrove cover. However, the high cost and limited spatial and temporal coverage of these applications have restricted their generalized use (Kuenzer et al. 2011; Rahman et al. 2013). In contrast, other satellite products such as those derived from NOAA AVHRR or SPOT VEGETATION provide a continuous coverage of vast regions of the planet, but their low spatial resolution (1–4 km) limits their capacity to record detailed changes in plant cover. A suitable compromise between spatial and temporal resolution is provided by the 250 and 500 m resolution imagery, recorded daily by MODIS (moderate-resolution imaging spectroradiometer), installed aboard the Terra and Aqua satellites.

Additionally, the calibration systems in MODIS allow the production of accurate geometric rectification, as well as cloud detection and atmospheric correction (Langner et al. 2007), resulting in the production of different land-cover specialized products, such as the 16-day composite vegetation indexes, that are widely used to analyze vegetation dynamics (Hall-Beyer 2003; Chéret and Denux 2011). Deriving information from these vegetation indexes is useful for analyzing variations in vegetation phenology and to detect trends of change, which are

✉ César Alejandro Berlanga-Robles
cesar@ciad.mx

¹ Doctorado en Ciencias Marinas, Departamento de Recursos del Mar, Centro de Investigación y de Estudios Avanzados del IPN, Km 6 Antigua Carretera a Progreso, CORDEMEX, 97310 Mérida, Yucatán, Mexico

² Centro de Investigación en Alimentación y Desarrollo A. C., Coordinación Regional Mazatlán, Av. Sábalo Cerritos s/n, 82112 Mazatlán, Sinaloa, Mexico

³ Departamento de Matemáticas, Universidad Autónoma Metropolitana-Iztapalapa, AP 55-534, Iztapalapa, 09340 Ciudad de México, Mexico

difficult to obtain with data from other satellites that have higher spatial resolution but lower temporal resolution.

Based on the above considerations, this study aimed to characterize the temporal and spatial patterns of mangrove canopies in a large coastal ecosystem, seasonally and over the long term. This research is based on the decomposition of a monthly time series (2001 to 2016) of the MODIS enhancement vegetation index (EVI) using principal component analysis (PCA).

Mangroves in Marismas Nacionales, the selected case study area, have been subject to various disturbance events, such as severe salt water intrusion caused by the opening of an artificial channel to connect the lagoon system with the Pacific Ocean, that have resulted in substantial erosion because of incorrect planning. In addition, hurricane occurrences, modifications in the local hydrology and a strong coastal dynamic (Berlanga-Robles and Ruiz Luna 2007; Blanco et al. 2011; De la Lanza and Hernández 2017) have resulted in the loss of approximately 14,000 ha of Marismas Nacionales mangrove cover over the last quarter of the twentieth century (Berlanga-Robles and Ruiz Luna 2007). Even when those impacts were

documented based on remote sensing analyses (De la Lanza et al. 1996; Kovacs et al. 2001; Berlanga-Robles and Ruiz Luna 2007), only the spatial changes were analyzed, but there is no updated information on this vegetation cover, considering both the distribution patterns and vegetation conditions, which is the purpose of the present study.

Methods

Study area

Marismas Nacionales is part of the Teacapan-Agua Brava lagoon system located in northwestern Mexico, between 21° 43' and 22° 59' N, and the 105° 08' and 106° 02' W. The system, a complex 186,400-ha mosaic of lagoons, mangroves and saltmarshes, is integrated with the Cerritos, Cañas, Agua Grande, Pescaderos and Grande de Mexcaltitan lagoons (Fig. 1). This system has the most extensive mangrove forest in the Mexican Pacific, consisting of the four main mangrove species reported in

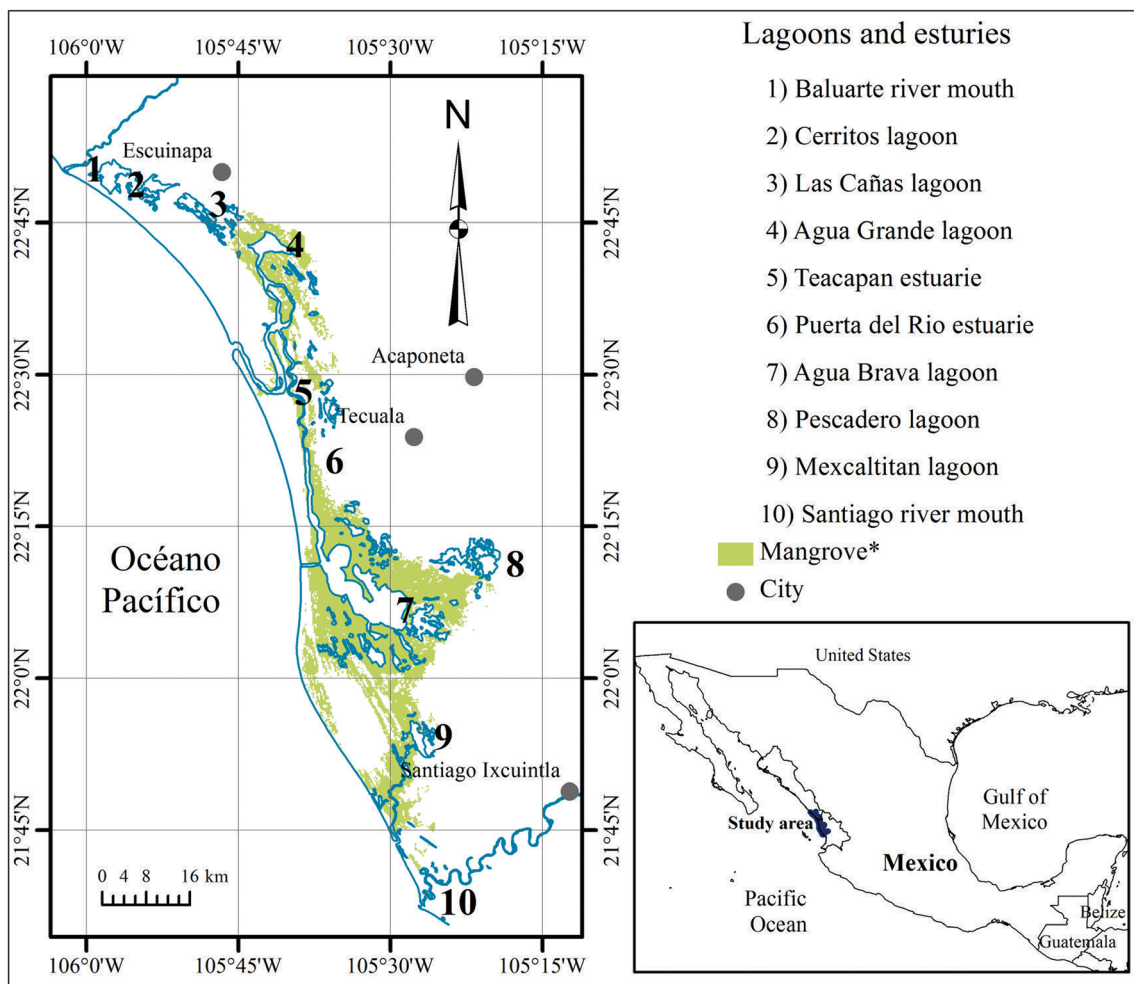


Fig. 1 Study area. Marismas Nacionales is in the Teacapan-Agua Brava lagoon system in northwest Mexico. *The mangrove area in 2000 estimated by Berlanga-Robles and Ruiz-Luna (2007) is shown in green

Mexico: *Laguncularia racemosa* (white mangrove), *Rhizophora mangle* (red mangrove), *Avicennia germinans* (black mangrove) and *Conocarpus erectus* (button mangrove) (Fig. 2), with a heterogeneous distribution dominated by white mangrove (De la Lanza et al. 1996). The climate in the region is A(w), warm and sub-humid with rain in the summer, with an average annual temperature of 24.7 °C and an average annual rainfall of 922 mm (Berlanga-Robles and Ruiz Luna 2007).

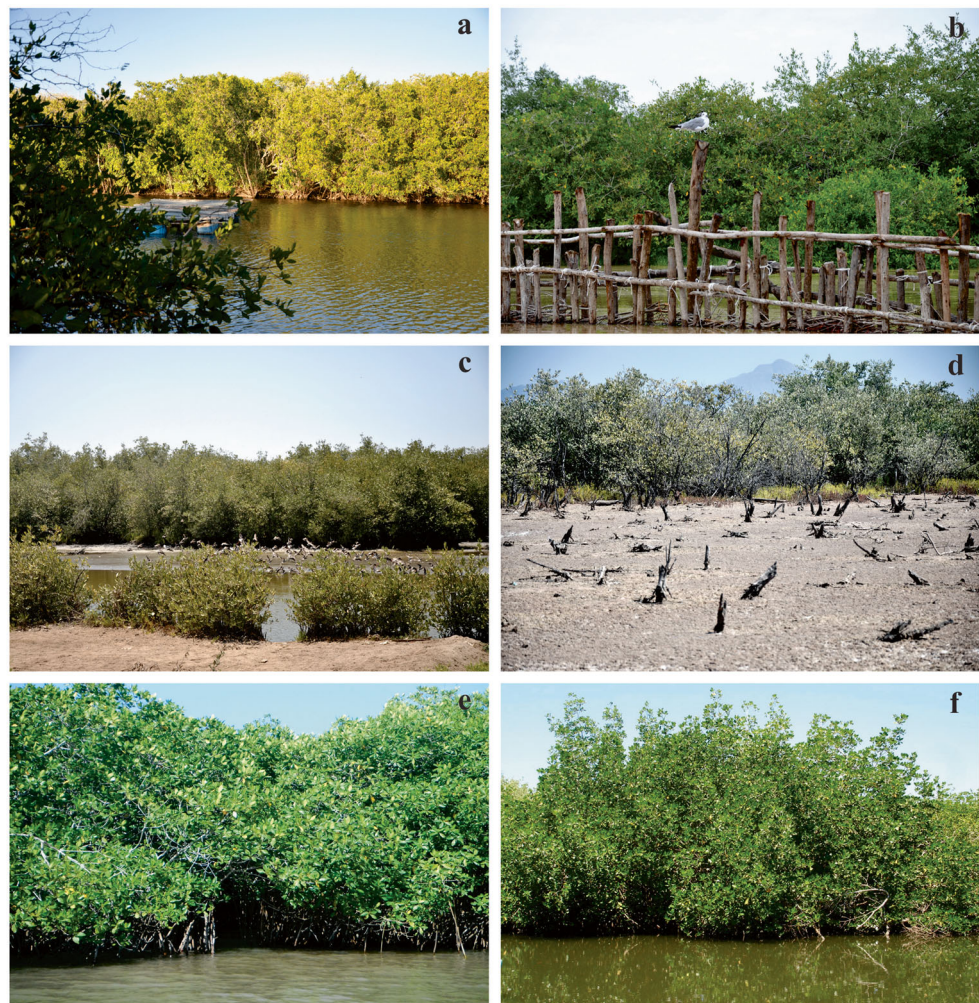
Data and preprocessing

A geographic information system (GIS) integrated 368 images of the band 250 m 16 EVI of the MOD13Q1 V.006 MODIS Terra products, corresponding to column 8 and line 6 (h08 / v06) of the MODIS sinusoidal network, downloaded from the Land Processes Distributed Active Archive Center site (LP DAAC: https://lpdaac.usgs.gov/data_access/data_pool). The enhanced vegetation index (EVI) was selected because it is highly sensitive to the dense canopy of dense forests, as well as resistant to the effects of dark soils, the atmosphere and residual clouds (Jiang et al. 2006, Rahman et al. 2013; Rossi et al. 2013). The

images were projected and windowed to the UTM 13Q (Datum WGS84) coordinates 374,175, 2,549,565 and 480,925, 2,392,065, and the original values of the pixels were rescaled (dividing them by 10,000) to the values of the vegetation index in the interval [0, 1] to generate a time series from 2001 to 2016 with 16-day intervals, which was subsequently reduced to monthly intervals, using the arithmetic mean.

Additionally, from a thematic map of the coastal wetlands of the Teacapan-Agua Brava Lagoon System in 2000 produced by Berlanga-Robles and Ruiz Luna (2007), a baseline map of the mangrove cover was edited to mask the other types of coverage and the mangrove patches less than 25 ha (the area of four pixels of 250 m) to limit the analysis of the time series to the areas covered by mangrove patches larger than 25 ha. The GIS was supplemented with meteorological data from the National Center for Environmental Prediction (NCEP), downloaded from Global Weather Data for SWAT (<http://globalweather.tamu.edu/>) from which monthly time series were generated, from January 2001 to July 2014 for the monthly maximum temperature, the monthly minimum temperature, the monthly precipitation, the accumulated

Fig. 2 Mangroves of Marismas Nacionales: **a** White mangrove at south of study area, **b** White and black mangroves in Mexcaltitan lagoon, **c** black mangrove at north of study area, **d** black mangrove with remains of dead tree close to Agua Grande Lagoon, **e** red mangrove and **f** white mangrove around of Mexcaltitan lagoon



precipitation (from the beginning of the hydrological year, in April, to the target month) and solar radiation.

Principal component analysis (PCA)

The monthly EVI time series was decomposed through a non-centralized normalized PCA with orientations in the S mode and the T mode. The geographic data time series is a four-dimensional space where x and y are the geographical space, z is the value of the data (e.g., vegetation index) and t is the time. In the PCA, there are six ways to decompose multidimensional data (O, P, Q, R, S and T), but only the S and T modes involve time and are applicable to geographic data if the space is considered as a collection of a unidirectional time series where each image represents a time interval. Orientation represents the way in which the time series of images is organized for analysis. In the S mode, the variables are samples in space and can identify recurrent temporal patterns in space. In the T mode, the variables are samples in time and allow the

identification of spatial patterns over time (Machado-Machado et al. 2011; Neeti and Eastman 2014).

The PCA was conducted using the TerrSet 18.3 program (Eastman 2015), producing scores and load component images in the S mode and principal components images in the T mode. The results interpretation in the S mode is from the load images and the score profiles, while in the T mode, the interpretation is based on the component images and the load profiles (Machado-Machado et al. 2011; Neeti and Eastman 2014; Eastman 2015). The significance of the monotonic trends of the scores and load profiles, as well as the profiles of the meteorological variables, were tested with the Mann-Kendall test (Neeti and Eastman 2011; Wagner et al. 2013), which was conducted using the “trend” package for R (Pholert 2017). Additionally, the relationship between the component scores and load profiles with the meteorological variable profiles was analyzed with the Kendall tau coefficient. This coefficient was selected because the data of the meteorological variables did not fit a normal distribution (Badii et al. 2014).

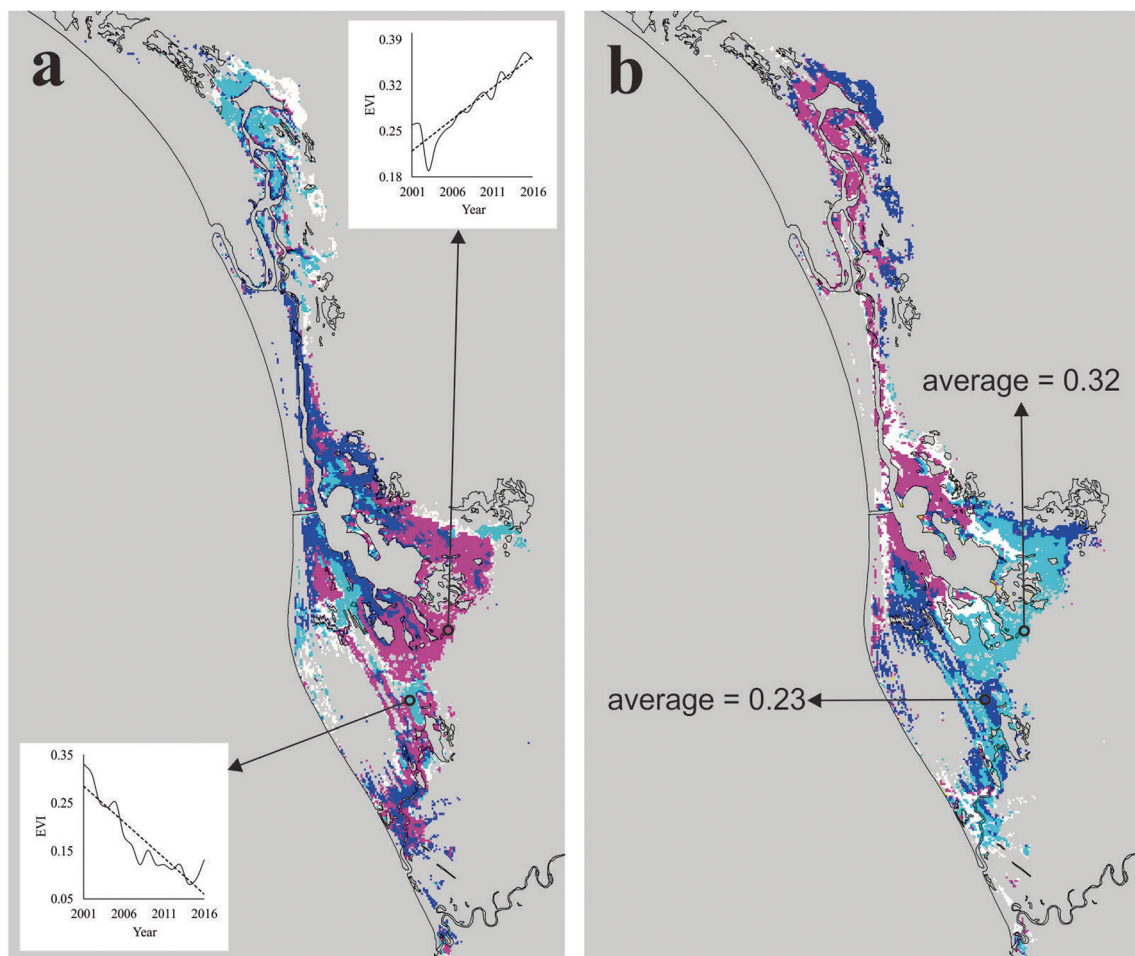


Fig. 3 False color composites of the first three component load images of the PCA in the S mode (a), and the first three component images of the PCA in the S mode (b). The S mode image shows the annual EVI profiles

for two mangrove areas, and the T mode image shows the EVI mean for all analyzed period of the two areas

Results

A mangrove surface of 72,675 ha of mangrove patches equal or greater to 25 ha was estimated from the line-base map, so that the PCA was executed for 97% of the total mangrove area of Marismas Nacionales (in 2000) as estimated by Berlanga-Robles and Ruiz Luna (2007). In the analyzed area, the EVI averages ranged from 0.18 to 0.33. The first three components of the analysis in the S mode explained 92.5%, 1.6% and 0.3% of the total variation. The false color composites of the load images of these components are the cyan and white areas where the EVI values tended to decrease and are the magenta and blue areas where they increase (Fig. 3a). On the other hand, the first three components of analysis in the T mode explained 96.9, 0.5% and 0.2% of the total variation, and the false color composites of their images were the cyan and violet areas where the EVI averages for the 16 analyzed years were highest, and the blue areas where the EVI averages were the lowest (Fig. 3b).

The first component in the S mode was related to the EVI seasonal changes, and its score profile described the vegetative phenological mangrove patterns. This profile presented the maximum between October and December and the minimum from May to June, such as the observed EVI profile for the analyzed area (Fig. 4a). Both profiles presented a positive

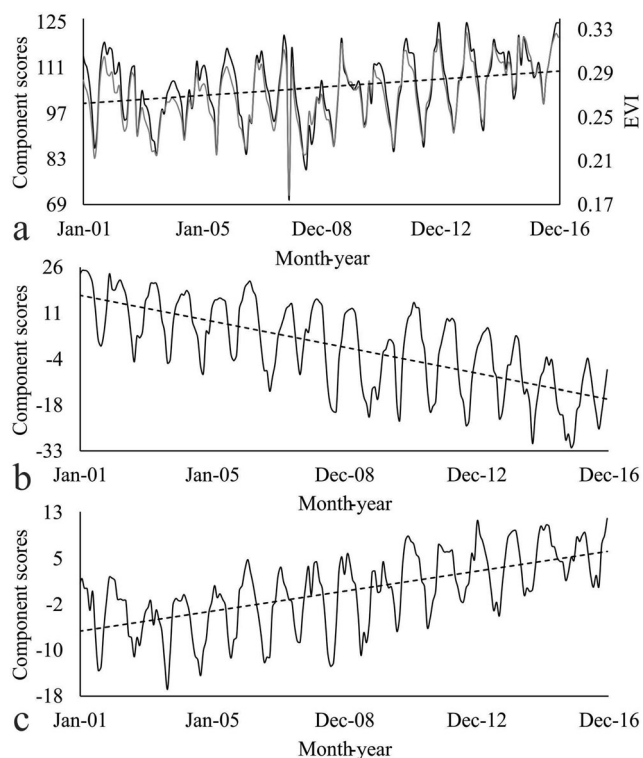


Fig. 4 Monthly component score profiles of the first (a), second (b) and third (c) components of the PCA in the S mode. In graph a, the gray line corresponds to the monthly EVI profile for all the mangrove areas analyzed

monotonic trend ($p = 0.00011$). The minimum values in the score profiles of the second component in the S mode were negative starting from 2002 (Fig. 4b), so that the profile showed a negative monotonic trend ($p = 2.2 \times 10^{-16}$). The load images of this component, filtered with green in the false color composite, recorded negative loads (correlations) in areas where the mangrove canopy tended to increase and positive loads where the mangrove canopy decreased; 348 pixels were recorded as significantly negative loads for $\alpha = 0.05$ and 475 para $\alpha = 0.1$. On the other hand, 1505 pixels had significant positive loads for 0.05 and 216 for $\alpha = 0.1$. Some significant positive loads are associated with dead mangroves. The scores of the third component in the S mode oscillated between negative and positive values until September 2013, but from there, with the exception of 1 month, they were only positives (Fig. 4c), and the score profile described a positive monotonic trend ($p = 3.2 \times 10^{-16}$). Its load images, filtered in red in the false color composite, recorded the highest values in areas where mangroves had a more closed canopy toward the end of the period analyzed.

The image of the first component in the T mode, filtered in blue in the false color composite, represents a vegetation gradient with the highest values corresponding to the mangroves with a closed canopy along the analyzed period. These mangroves with closed canopies were concentrated around the Agua Brava lagoon and south of the study area, while the lowest values associated with mangroves with open canopies

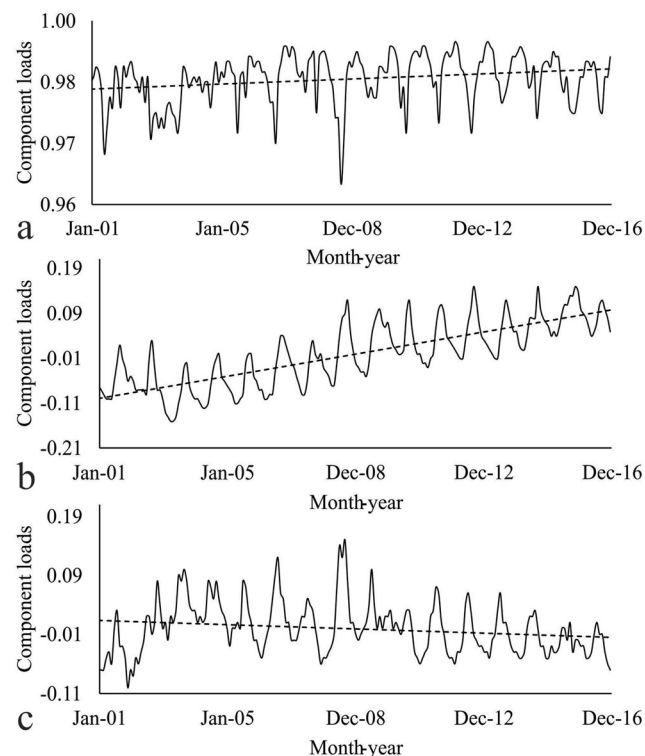


Fig. 5 Monthly component load profiles of the first (a), second (b), and third (c) components of the PCA in the T mode

were mainly located in the north. The load profiles of this component presented the maximum in the spring and the minimum in the autumn (Fig. 5a), describing a positive monotonic trend ($p = 8.54 \times 10^{-5}$). The second and third components in the T mode represented spatial gradients where the major vegetation density was in the beginning or end of the time series. The load profiles of second component (Fig. 5b) had a positive monotonic trend ($p = 2.2 \times 10^{-16}$), while that of the third component (Fig. 5c) was negative ($p = 0.00005$).

Related to meteorological variates, the monthly maximum temperature presented a negative monotonic trend ($p = 1.6 \times 10^{-13}$), the monthly minimum temperature presented a positive trend ($p = 2 \times 10^{-6}$), and the accumulated precipitation also presented a positive trend ($p = 0.00028$), while the monthly precipitation ($p = 0.8$) and monthly average solar radiation ($p = 0.9$) did not present any trends (Fig. 6). The score profile of the first component in the S mode that described the

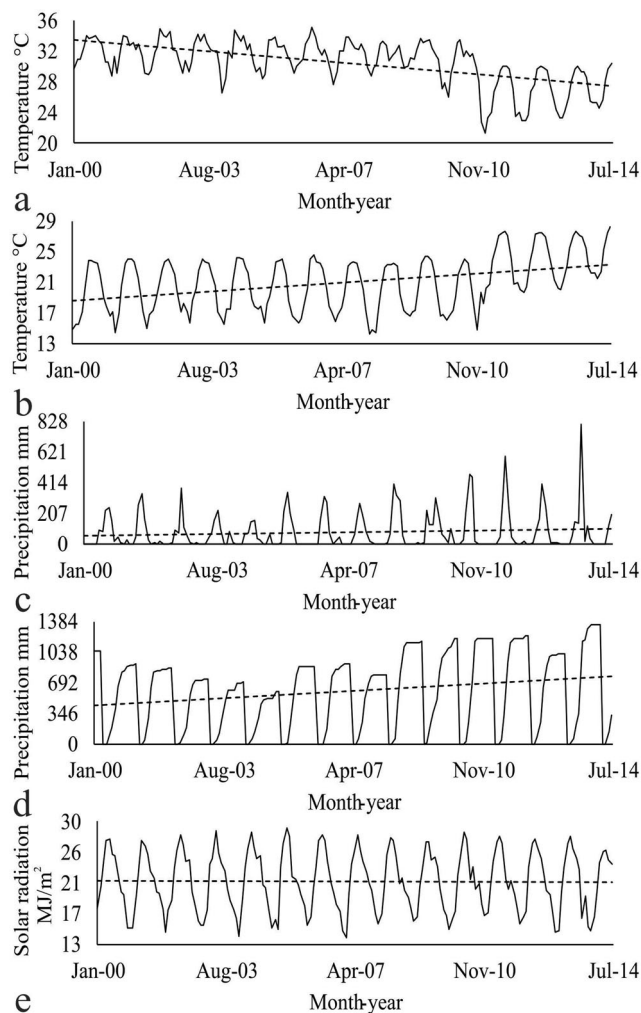


Fig. 6 Monthly profiles of the five meteorological variables in Marismas Nacionales, Mexico. **a** Maximum monthly temperature, **b** minimum monthly temperature, **c** monthly precipitation, **d** accumulated precipitation and **e** monthly average solar radiation

seasonal mangrove canopy changes had a significant correlation ($\alpha = 0.05$ and $n = 163$) with the maximum temperature, accumulated precipitation and the solar radiation. On the other hand, the score profiles of the third component and the load profiles of the first three components in the T mode had significant correlations with both temperature and monthly precipitation (Table 1).

Discussion

MODIS vegetation indices have been widely used to study vegetation dynamics and productivity at regional and global scales (Huete et al. 2002). However, mangrove studies supported with these data are scarce because their spatial resolution (minimum 250 m) is considered a limitation to conducting reliable and accurate analyses, based on the concept that mangroves are located in small patches or strips extending along rivers (Giri et al. 2015). Nevertheless, the use of the MODIS vegetation indices has allowed us to analyze the impact of natural and anthropogenic perturbations, as well as monitoring the variations in canopy cover in mangroves formed by patches of several hectares and with a regional distribution (Rogan et al. 2011; Vázquez 2012; Rahman et al. 2013; Rossi et al. 2013). In this sense, in 2000, 97% of the mangrove area of Marismas Nacionales was distributed in patches equal or greater to 25 ha (4 pixels of MOD13Q1 products). Based on the time continuity of these products, it was possible to identify the seasonal and long-term mangrove variations, which were otherwise impossible to detect with remote sensing data that had greater spatial resolution but limited temporal regularity.

Mangroves are perennial vegetation assemblages; however, they have phenological vegetative changes that are characterized by a strong climate component, where higher rates of leaves sprouting and litterfall are related to temperature variations (Gwada et al. 2000; Mehlig 2006; Pastor-Guzman et al. 2018). In Marismas Nacionales, the litterfall intensifies at the end of the dry season, when the deficit between evaporation and precipitation and the salinity are at their highest levels (Flores-Verdugo et al. 1990). The annual cycle of the canopy described by the S mode first component score profiles is consistent with the vegetative phenology patterns of the mangrove species located in the study area. The maximum vegetation vigor occurred during the autumn, 4 or 5 months ahead of the dry season, when the maximum temperature and solar radiation started to decrease, and accumulated precipitation almost reaches its maximum.

During the last quarter of the past century, the mangroves of Marismas Nacionales were subject to different natural and anthropogenic perturbation events, resulting in an average annual rate of deforestation of 0.64%, one of the highest rates registered in northwestern Mexico (Berlanga-Robles and Ruiz Luna 2007). In this study, the analysis was not focused on

Table 1 Kendall tau correlation between the principal component scores and load profiles and the meteorological variable profiles

Meteorological variable	Components					
	PCA mode S			PCA mode T		
	PC1	PC2	PC3	PC1	PC2	PC3
Tau						
Maximum temperature	-0.29	0.09	-0.46	-0.32	-0.25	0.31
Minimum temperature	-0.18	-0.46	-0.27	-0.29	0.35	0.33
Monthly precipitation	-0.10	-0.43	-0.47	-0.48	0.29	0.43
Accumulated precipitation	0.40	-0.20	0.23	0.12	0.32	-0.21
Solar radiation	-0.42	0.16	-0.06	0.01	-0.20	0.11
<i>p</i> values						
Maximum temperature	0.0054	1.0000	0.0000	0.0009	0.0398	0.0022
Minimum temperature	0.4487	0.0000	0.0166	0.0058	0.0002	0.0006
Monthly precipitation	1.0000	0.0000	0.0000	0.0000	0.0044	0.0000
Accumulated precipitation	0.0000	0.2139	0.0659	1.0000	0.0009	0.1427
Solar radiation	0.0000	0.6184	1.0000	1.0000	0.2126	1.0000

The bold values were significant at $\alpha = 0.05$ ($n = 163$)

directly measuring the land-cover and land-use changes; therefore, the results cannot inform the previously mentioned deforestation rate, however, they provide evidence that degradation of this forest persists. Approximately 11,000 ha, 15% of the analyzed area, correspond to mangroves that have notably diminished canopies (with significant positive loads for the S mode second component). Mangroves characterized by a decrease in canopy were concentrated in zones where Blanco et al. (2011) reported mangrove degradation caused by fluvial and tidal flow alterations and where De la Lanza et al. (1996) reported predominance of *A. germinans*.

The PCA indicated that 7% of the mangroves registered considerable increments in their canopies. These mangroves are located south of Agua Brava Lagoon, in tidal basins with no deterioration or with sedimentary fluvial flow increases (Blanco et al. 2011) and in zones with patches dominated by *L. racemosa* or by *L. racemosa* and *R. mangle* (De la Lanza et al. 1996). According to Berlanga-Robles and Ruiz Luna (2007), the mangroves of Marismas Nacionales reached an equilibrium at the end of the past century, and after this time, they were subject to high perturbation events. In general, during this century, these mangroves have maintained this equilibrium, as has been shown for the past three quinquennial, where more than 80% of the mangroves have remained or increased their canopies, and the EVI profile has a positive trend. Consequently, almost all canopy variations in the analyzed period were due to seasonal changes associated with the vegetative phenology of the mangrove species and not associated with land-cover changes or dead mangroves.

In that regard, Rioja-Nieto et al. (2017), found that accumulated precipitation and maximum temperature are the major environmental drivers of the long-term changes in the

mangroves on the coastline of Yucatan, Mexico. However, in this study, it was found that these two variables, and solar radiation, were associated with the principal components that described the seasonal changes, whereas the components that described the medium and long-term changes were more correlated with minimum temperatures and monthly precipitation. Also, De la Lanza and Hernández (2017) noted a decrease in precipitation of 3% in the study area (not detected in this study because a shorter time series was analyzed), which led to changes in salinity, temperature, nutrient concentrations and circulation patterns, affecting mangrove distribution and health, so that some of the negative trends detected may be due to precipitation anomalies.

Many ecosystem services provided by mangroves depend on their high net primary productivity, which in turn is a function of the canopy structure, that maintains a continuous litter production, later assimilated into the food webs, contributing to soil formation or exported to adjacent coastal waters (Sukardjo et al. 2013). Therefore, studying mangrove phenology is fundamental to estimate productivity and photosynthetic biomass of these ecosystems, but also to model trends of change and to detect variations in the forests health, allowing the development of conservation and restoration strategies without interference on the natural regeneration (Agraz et al. 2011).

In addition, the present approach, decomposing time series of canopy structure indicators (vegetation indices), allow the analyzes of mangroves phenology at different spatial scales, giving technical elements to characterize the interactions between vegetation and climate and to understand their contribution to biogeochemical cycles (Pastor-Guzman et al. 2018).

With this technical approach, it is possible to distinguish long-term changes from seasonal ones, so the land cover and

land use change studies can be improved with more accurate estimates and by adding indicators of impacts on the structure of forest. In Marismas Nacionales, despite of the detected negative trends, the outcomes of this study suggest a certain recovery and stability of the mangrove forest canopy. The PCA allows us to identify vulnerable, resilient and resistant mangrove elements, based on the study of De la Lanza et al. (1996), and our experience in the study area allow us to identify *A. germinans* as the most vulnerable species. The images of different components and their false color composites (available upon request to the corresponding author) are a support tool that can help define different conservation strategies for each of these mangrove elements, giving special care in the areas where negative trends were detected and focus new studies to identify and evaluate the impacts of different change drives.

Acknowledgements The authors thank the National Council for Science and Technology (CONACYT) for financing the SEP-CONACYT Basic Science Project 157533 “Modeling the relationships between the spatial patterns of the mangrove forest and the distribution and abundance of penaeid shrimp in the Teacapán-Agua Brava lagoon system, Mexico”, and for the grant 748017 to Marta R. Nepita. The MODQ131 products were retrieved online, courtesy of NASA EOSDIS Land Processes Distributed Active Archive Center (LP DAAC), USGS/Earth Resources Observation and Science (EROS) Center, Sioux Falls, South Dakota, DAAC. The climate data used in this study were courtesy of the National Center for Environmental Prediction (NCEP), Global Weather Data for SWAT.

References

- Agraz HCM, García ZC, Iriarte-Vivar S, Flores-Verdugo FJ, Moreno CP (2011) Forest structure, productivity and species phenology of mangroves in the La Mancha lagoon in the Atlantic coast of Mexico. *Wetl Ecol Manag* 19:273–293. <https://doi.org/10.1007/s11273-011-9216-4>
- Badii MH, Guillen A, Lugo SOP, Aguilar GJJ (2014) Correlación no-paramétrica y su aplicación en la Investigaciones científica. *Int J Good Consc* 9:31–40. <http://www.spentamexico.org/v9-n2/A5.9%282%2931-40.pdf>. Accessed 14 June 2018
- Berlanga-Robles CA, Ruiz Luna A (2007) Análisis de las tendencias de cambio del bosque de mangle del sistema lagunar Teacapán-Agua Brava, México. Una aproximación con el uso de imágenes de satélite Landsat. *Univ Cienc* 23:29–46
- Blanco y Correa M, Flores VF, Ortiz PMA, de la Lanza EG et al (2011) Análisis Funcional de Marismas Nacionales. Universidad Autónoma de Nayarit, México
- Chéret V, Denux J-P (2011) Analysis of MODIS NDVI time series to calculate indicators of Mediterranean forest fire susceptibility. *GISCI REMOTE SENS* 48:171–194. <https://doi.org/10.2747/1548-1603.48.2.171>
- De la Lanza EG, Hernández PS (2017) Natural and induced space/time environmental changes in the Teacapán-Agua Brava lagoon system, NW Mexico. *JAMB* 5:00140. <https://doi.org/10.15406/jamb.2017.05.00140>
- De la Lanza EG, Sánchez S, Sorani V, Bojórquez T (1996) Características geológicas, hidrológicas, y del manglar en la planicie costera de Nayarit, México. *Invest Geog* (32):33–54
- Eastman JR (2015) TerrSet. Geospatial monitoring and modelling system. Tutorial. Clark Labs, Massachusetts
- Flores-Verdugo F, González-Farías F, Ramírez-Flores O, Amezcua-Linares F, Yáñez-Arancibia A, Alvarez-Rubio M, Day JW (1990) Mangrove, aquatic primary productivity, and fish community dynamics in Teacapán-Agua Brava lagoon-estuarine system (Mexican Pacific). *Estuaries* 13:219–230
- Giri C (2016) Observation and monitoring of mangrove forests using remote sensing: opportunities and challenges. *Remote Sens* 783:1–8. <https://doi.org/10.3390/rs8090783>
- Giri C, Ochieng E, Tieszen LL, Zhu Z, Singh A, Loveland T, Masek J, Duke N (2011) Status and distribution of mangrove forests of the world using earth observation satellite. *Glob Ecol Biogeogr* 20:154–159. <https://doi.org/10.1111/j.1466-8238.2010.00584.x>
- Giri C, Long J, Abbas S, Murali RM, Qamer FM, Pengra B, Thau D (2015) Distribution and dynamics of mangrove forests of South Asia. *J Environ Manag* 148:101–111. <https://doi.org/10.1016/j.jenvman.2014.01.020>
- Gwada P, Makoto T, Uezu Y (2000) Leaf phenological traits in the mangrove *Kandelia candel* (L.) Druce. *Aquat Bot* 68:1–14. [https://doi.org/10.1016/S0304-3770\(00\)00109-1](https://doi.org/10.1016/S0304-3770(00)00109-1)
- Hall-Beyer (2003) Comparison of single-year and multiyear NDVI time series principal components in cold temperate biomes. *IEEE Trans Geosci Remote Sens* 41:1–8. <https://doi.org/10.1109/TGRS.2003.817274>
- Huete A, Didan K, Miura T, Rodriguez EP, Gao G, Ferreira XL (2002) Overview of the radiometric and biophysical performance of the MODIS vegetation indices. *Remote Sens Environ* 83:195–213. [https://doi.org/10.1016/S0034-4257\(02\)00096-2](https://doi.org/10.1016/S0034-4257(02)00096-2)
- Jiang ZY, Huete AR, Chen J, Chen YH, Li J, Yan GJ, Zhang XY (2006) Analysis of NDVI and scaled difference vegetation index retrievals of vegetation fraction. *Remote Sens Environ* 101:366–378. <https://doi.org/10.1016/j.rse.2006.01.003>
- Kovacs JM, Wang J, Blanco-Correa M (2001) Mapping disturbances in mangrove forest using multi-date Landsat TM imagery. *Environ Manag* 27:763–766. <https://doi.org/10.1007/s002670010186>
- Kuenzer C, Bluemel A, Gebhardt S, Vo Quoc T, Dech S (2011) Remote sensing of mangrove ecosystems: a review. *Remote Sens* 3:878–928. <https://doi.org/10.3390/rs3050878>
- Langner A, Miettinen J, Siegert F (2007) Land cover change 2002–2005 in Borneo and the role of fire derived from MODIS imagery. *Glob Chang Biol* 13:2329–2340. <https://doi.org/10.1111/j.1365-2486.2007.01442.x>
- Machado-Machado EA, Neeti N, Eastman JR, Chen H (2011) Implications of space-time orientation for principal components analysis of earth observation image time series. *Earth Sci Inf* 4: 117–124. <https://doi.org/10.1007/s12145-011-0082-7>
- Mehlig U (2006) Phenology of red mangrove, *Rhizophora mangle* L, in the Caeté estuary, Pará, equatorial Brazil. *Aquat Bot* 84:158–164. <https://doi.org/10.1016/j.aquabot.2005.09.007>
- Neeti N, Eastman JR (2011) A contextual Mann-Kendall approach for assessment of trend significance in image time series. *Trans GIS* 15: 599–611. <https://doi.org/10.1111/j.1467-9671.2011.01280.x>
- Neeti N, Eastman JR (2014) Novel approaches in extended principal component analysis to compare spatio-temporal patterns among multiple image series. *Remote Sens Environ* 148:84–96. <https://doi.org/10.1016/j.rse.2014.03.015>
- Pastor-Guzman J, Dash J, Atkinson PM (2018) Remote sensing of mangrove forest phenology and its environmental drivers. *Remote Sens Environ* 205:71–84. <https://doi.org/10.1016/j.rse.2017.11.009>
- Pholert T (2017) Package ‘trend’. On line: <https://cran.r-project.org/web/packages/trend/trend.pdf>. Accessed 14 Dec 2017
- Rahman AF, Dragoni D, Didan K, Barreto-Munoz A, Hutabarat JA (2013) Detecting large scale conversion of mangroves to aquaculture with change point and mixed-pixel analyses of high-fidelity

- MODIS data. *Remote Sens Environ* 130:96–107. <https://doi.org/10.1016/j.rse.2012.11.014>
- Rioja-Nieto R, Barrera-Falcón E, Torres-Irineo E, Mendoza-González G, Cuervo-Robayo AP (2017) Environmental drivers of decadal change of a mangrove forest in the north coast of the Yucatan peninsula, Mexico. *J Coast Conserv* 21:167–175. <https://doi.org/10.1007/s11852-016-0486-0>
- Rogan J, Schneider L, Christman Z, Millones M, Lawrence D, Schmoor B (2011) Hurricane disturbance mapping using MODIS EVI data in the southeastern Yucatán, Mexico. *Remote Sens Lett* 2:259–267. <https://doi.org/10.1080/01431161.2010.520344>
- Rossi E, Rogan J, Schneider L (2013) Mapping forest damage in northern Nicaragua after hurricane Felix (2007) using MODIS enhanced vegetation index data. *GISCI REMOTE SENS* 50(4):171–194. <https://doi.org/10.1080/15481603.2013.820066>
- Sukardjo S, Alongi DM, Kusmana C (2013) Rapid litter production and accumulation in Bornean mangrove forest. *Ecosphere* 4:79. <https://doi.org/10.1890/ES13-00145.1>
- Vázquez LAD (2012) Exploración de Parámetros Biofísicos con Series de Tiempo de Productos MODIS y Estimación de Biomasa con Imágenes de Radar en los Manglares de Laguna Pom Atasta, Campeche y Laguna Agua Brava, Nayarit, México. Dissertation, Centro de Investigaciones en Geografía y Geomática “Ing. Jorge L. Tamayo”, A.C
- Wagner APL, Fontana DC, Fraisee C, Weber RJ, Hasenack H (2013) Tendências temporais de índices de vegetação nos campos do Pampa do Brasil e do Uruguai. *Pesq Agrop Brasileira* 48:1192–1200. <https://doi.org/10.1590/S0100-204X2013000900002>

Publisher's note Springer Nature remains neutral with regard to jurisdictional claims in published maps and institutional affiliations.